Palmitoylation of caveolin-1 is regulated by the same DHHC acyltransferases that modify steroid hormone receptors

Received for publication, May 25, 2018, and in revised form, August 27, 2018 Published, Papers in Press, August 29, 2018, DOI 10.1074/jbc.RA118.004167

Katherine R. Tonn Eisinger[‡§], Kevin M. Woolfrey[¶], Samuel P. Swanson[‡], Stephen A. Schnell[‡], John Meitzen[‖], Mark Dell'Acqua[¶], and Paul G. Mermelstein[‡§1]

From the [‡]Department of Neuroscience and the [§]Graduate Program in Neuroscience, University of Minnesota, Minneapolis, Minnesota 55455, the [¶]Department of Pharmacology, University of Colorado Denver, Aurora, Colorado 80045, and the [‖]Department of Biological Sciences, North Carolina State University, Raleigh, North Carolina 27695

Edited by George M. Carman

Palmitoylation is a reversible post-translational addition of a 16-carbon lipid chain involved in trafficking and compartmentalizing target proteins. It is important for many cellular functions, including signaling via membrane-localized estrogen receptors (ERs). Within the nervous system, palmitoylation of ERα is necessary for membrane surface localization and mediation of downstream signaling through the activation of metabotropic glutamate receptors (mGluRs). Substitution of the single palmitoylation site on ERα prevents its physical association with the integral membrane protein caveolin-1 (CAV1), required for the formation of the ER/mGluR signaling complex. Interestingly, siRNA knockdown of either of two palmitoyl acyltransferases, zinc finger DHHC type–containing 7 (DHHC7) or DHHC21, also eliminates this signaling mechanism. Because ERα has only one palmitoylation site, we hypothesized that one of these DHHCs palmitoylates CAV1. We investigated this possibility by using an acyl–biotin exchange assay in HEK293 cells in conjunction with DHHC overexpression and found that DHHC7 increases CAV1 palmitoylation. Substitution of the palmitoylation sites on CAV1 eliminated this effect but did not disrupt the ability of the DHHC enzyme to associate with CAV1. In contrast, siRNA-mediated knockdown of DHHC7 alone was not sufficient to decrease CAV1 palmitoylation but rather required simultaneous knockdown of DHHC21. These findings provide additional information about the overall influence of palmitoylation on the membrane-initiated estrogen signaling pathway and highlight the importance of considering the influence of palmitoylation on other CAV1-dependent processes.

Palmitoylation is the post-translational addition of a 16-carbon lipid chain that increases protein hydrophobicity. *S*-Palmitoylation, occurring via thioester bonds at cysteine residues, is reversible, making it an important means of dynamic cellular regulation (1). Palmitoylation has been implicated in many processes, including regulation of protein conformation, membrane association, protein–protein interactions, and compartmentalization and trafficking within cells (2–5). Through these mechanisms, palmitoylation can modulate a variety of signal transduction pathways. One such pathway is membrane-initiated estradiol signaling, which occurs in the nervous system via estrogen receptor (ER)[2] interactions with metabotropic glutamate receptors (mGluRs). This interaction leads to estradiol-mediated mGluR signaling independent of glutamate (6, 7). Neuronal ER/mGluR signaling in females underlies the effects of estradiol on learning and memory, nociception, motor control, sexual receptivity, and heightened responses to drugs of abuse (8). Recent findings also implicate ER/mGluR signaling in the male quail brain (9, 10) and the male and female rodent cerebellum (11). The ERs that signal through mGluRs are the same proteins that regulate gene expression in the nuclei of cells, except they have undergone palmitoylation, thereby promoting their trafficking to the plasma membrane (12, 13). Two specific palmitoyl acyltransferases, DHHC7 and DHHC21, have been identified as crucial for ER palmitoylation; disrupting the expression of either enzyme will eliminate membrane ER localization (14) and neuronal ER/mGluR signaling (7). These results are somewhat surprising. Because there is only one palmitoylation site on ERs, it has been unclear why knockdown of either enzyme would disrupt ER trafficking and not require inhibition of both DHHC7 and DHHC21.

The fact that ER/mGluR interactions do not occur spontaneously but rather require caveolin proteins to physically associate (15–17) may provide clues to resolve this discrepancy. Caveolins are integral membrane proteins enriched in lipid rafts and are responsible for creating microdomains of signaling proteins, including mGluRs (18, 19). There are three caveolin isoforms with specific expression patterns and interaction partners. Caveolin proteins are also palmitoylated (20), although the DHHC enzymes responsible are unknown. In this study, we examined the palmitoylation of caveolin-1 (CAV1), as it clusters group I mGluRs with estrogen receptor α (ERα) (15, 21).

This work was supported by National Institutes of Health Grants R01DA035008 and R01DA041808 (to P. G. M.), R01NS040701 (to M. L. D.), and R01MH109471 (to J. M.). K. R. T. E. was supported by National Institutes of Health Grant T32DA007234 (to P. G. M.). The authors declare that they have no conflicts of interest with the contents of this article. The content is solely the responsibility of the authors and does not necessarily represent the official views of the National Institutes of Health.

This article contains Fig. S1.

[1] To whom correspondence should be addressed: Dept. of Neuroscience, University of Minnesota, Minneapolis, MN 55455. Tel.: 612-624-8977; E-mail: pmerm@umn.edu.

[2] The abbreviations used are: ER, estrogen receptor; mGluR, metabotropic glutamate receptor; CAV1, caveolin-1; 2-Br, 2-bromopalmitate; qPCR, quantitative PCR; CREB, cAMP-responsive element-binding protein; pCREB, phosphorylated CREB; CHX, cycloheximide; HA, hemagglutinin; MT, mutant; ABE, acyl–biotin exchange; NEM, *N*-ethylmaleimide; TIRF, total internal reflectance fluorescence.

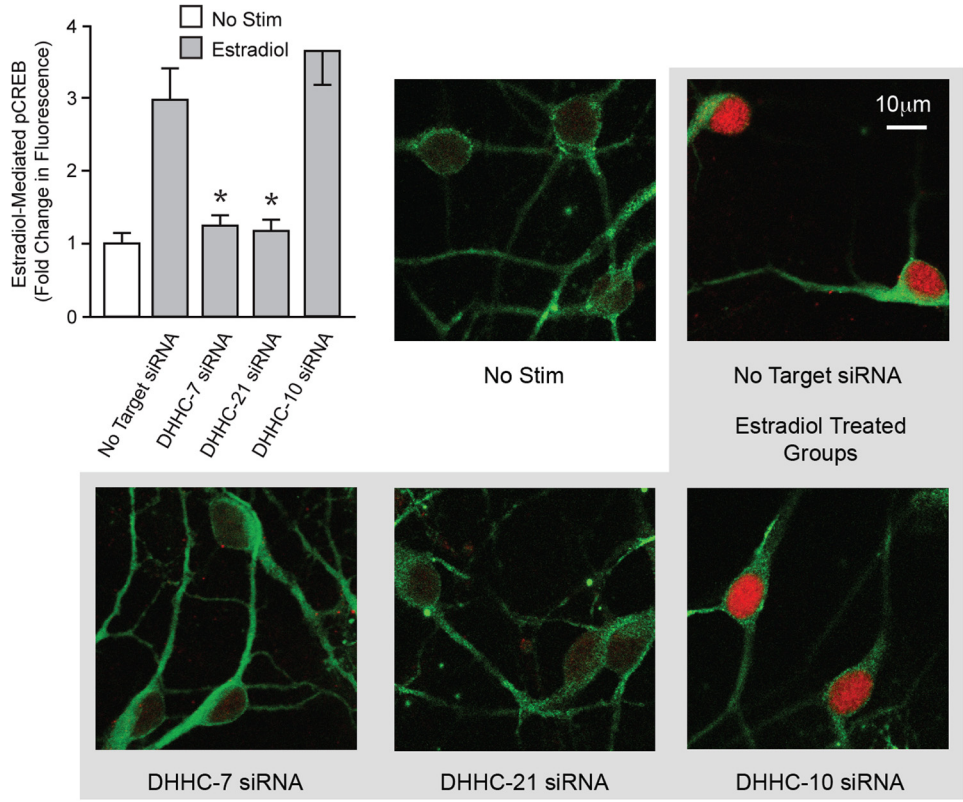

Figure 1. DHHC7 and DHHC21 are required for estradiol-induced CREB phosphorylation. Primary cultures of female-derived rat hippocampal neurons were transfected with control siRNAs or those targeting zDHHC7, zDHHC21, or zDHHC11 (DHHC10). 48 h later, cultures were stimulated for 5 min with 1 nM 17β-estradiol (*gray bars*) or vehicle (*white bar*) prior to immunocytochemical processing for CREB phosphorylation (pCREB, *red*; microtubule-associated protein 2, *green*). Estradiol-induced pCREB was eliminated when expression of either DHHC7 or DHHC21 was disrupted. *, $p < 0.01$ *versus* no target siRNA estradiol-treated group. *No Stim*, no stimulation.

We find that the same enzymes responsible for ER palmitoylation can also affect CAV1 palmitoylation, supporting our hypothesis that the same DHHC enzymes cooperate to facilitate surface membrane signaling.

Results

DHHC7 and DHHC21 are required for the rapid effects of estradiol on CREB phosphorylation

Estrogen receptors have a single palmitoylation site contained within a palmitoylation motif conserved across steroid hormone receptors. Of the 23 palmitoyl acyltransferase enzymes, two have been found essential for palmitoylation of these receptors, DHHC7 and DHHC21. These two enzymes regulate estrogen receptor trafficking in MCF-7 cells (14) and membrane estrogen receptor signaling in neurons (7). Here, we confirm that these enzymes are required for rapid membrane-initiated estradiol signaling. To do so, we transfected cultured hippocampal neurons derived from female rat pups with siRNAs targeting genes zDHHC7 and zDHHC21 and subjected the neurons to a 5-min estradiol stimulation. Normally, this stimulation increases nuclear CREB phosphorylation, as was the case with a nontargeting control siRNA or when targeting zDHHC11, which contains the transcript for DHHC10, an enzyme that does not palmitoylate steroid hormone receptors (Fig. 1). In contrast, disrupting expression of either DHHC7 or DHHC21 abolished the estradiol-induced CREB phosphorylation. siRNA targeting DHHC7 produced a 92% decrease in mRNA ($p < 0.05$, as measured via RT-qPCR), without affecting DHHC21 (13%, not significant). Reciprocally, siRNA targeting DHHC21 produced a 72% decrease in its mRNA ($p < 0.05$, as measured via RT-qPCR), without affecting DHHC7 (10%, not significant).

CAV1 is endogenously palmitoylated

Given that estrogen receptors have only one palmitoylation site, but knockdown of *either* DHHC7 or DHHC21 eliminated estradiol-induced CREB phosphorylation, we sought to ascertain whether these enzymes also play a role in CAV1 palmitoylation, because CAV1 is essential for ER/mGluR coupling. To test our hypothesis that DHHC7 and/or DHHC21 can affect CAV1 palmitoylation, we first validated the specificity of the CAV1 antibody used for quantification by Western blotting samples from WT or CAV1 KO mice (22). We found that the antibody used in these studies detected a band of the correct size (approximately 22 kDa) in WT mice but did not detect a similar band in KO mice (Fig. 2*A*). We next determined whether CAV1 is palmitoylated under steady-state conditions in HEK293 cells using an acyl–biotin exchange assay (Fig. 2*B*). We found that CAV1 is palmitoylated under unstimulated conditions (Fig. 2*B*, *first two lanes*). We next overexpressed Myc-tagged DHHC7, DHHC21, and DHHC10 in these cells (Fig. 2*B*, *six right-hand lanes*), hypothesizing that DHHC7 or DHHC21 would increase CAV1 palmitoylation and that DHHC10 would have no effect. Counter to our prediction, none of the overex-

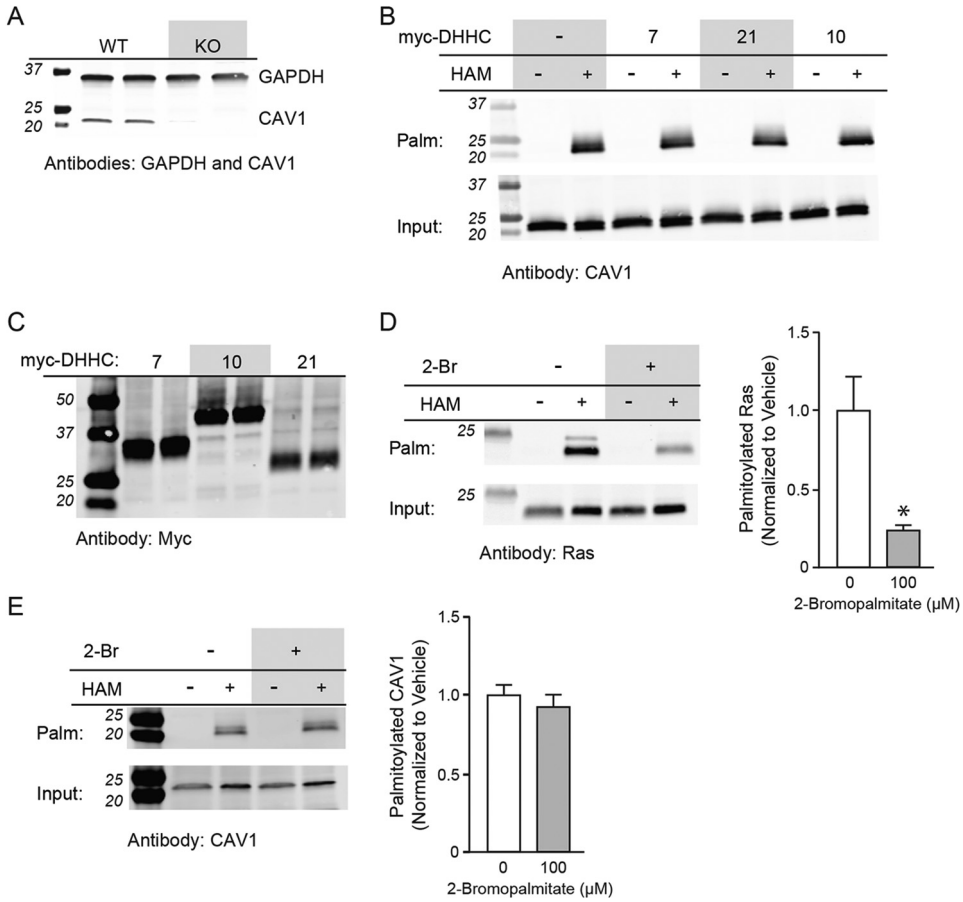

Figure 2. Endogenous CAV1 exhibits palmitoylation permanence. *A*, validation of the CAV1 antibody using striatal tissue from two WT *versus* two CAV1 knockout mice. *B*, detection of CAV1 in the presence, but not the absence, of hydroxylamine (*HAM*) in the ABE assay indicates endogenous CAV1 palmitoylation (*Palm*) in HEK293 cells. Endogenous CAV1 palmitoylation was unaffected by DHHC7, DHHC21, or DHHC10 overexpression. *C*, validation of overexpression of Myc-tagged DHHC7, DHHC10, and DHHC21; two samples are shown of each. *D* and *E*, overnight treatment with 100 μM 2-Br decreased palmitoylation of Ras, but not of CAV1.

pressed enzymes increased palmitoylation of endogenous CAV1. As a control, we verified expression of the Myc-DHHC proteins via Western blotting (Fig. 2*C*).

Although this finding was initially surprising, previous reports suggested a possible explanation. Although CAV1 palmitoylation is technically reversible in that it occurs through *S*-palmitoylation (a bond that would be subject to depalmitoylation), Parat and Fox found that CAV1 palmitoylation is, in fact, an essentially permanent modification (23). It was hypothesized that once palmitoylated, these sites are immediately embedded in the membrane and become inaccessible to depalmitoylating enzymes. To determine whether this might explain our results, we treated cells with the pan-palmitoylation inhibitor, 2-bromopalmitate (2-Br) overnight. We used small GTPase Ras proteins as a positive control because they are ubiquitously expressed and dynamically palmitoylated (24–26). Although 2-Br decreased palmitoylated Ras protein levels by ~80% (Fig. 2*D*, $t(4) = 3.564$, $p < 0.05$), 2-Br did not decrease CAV1 palmitoylation levels (Fig. 2*E*, $t(4) = 0.7528$, $p = 0.49$). Thus, it is likely that the time scale of our experiments was insufficient to detect any changes in endogenous CAV1 palmitoylation.

For further experiments, we needed to isolate a newly translated pool of CAV1. One strategy to do so would be to halt protein synthesis with cycloheximide (CHX) and then monitor changes in palmitoylation of newly translated protein following release from CHX treatment. However, we found that overexpression of DHHC7 or DHHC21 eliminated the decrease in CAV1 palmitoylation following CHX treatment that was observed in nontransfected cells (Fig. S1). Therefore, although this suggested a stabilization effect, it was not a viable approach for determining DHHC-substrate relationships. This led us to overexpress CAV1 to make a pool of newly synthesized CAV1 available and overcome this limitation yet still monitor the initial palmitoylation of the protein.

DHHC7 increases HA–CAV1 palmitoylation

In the remaining experiments, HA-tagged CAV1 was transfected into HEK293 cells to provide a newly expressed pool of CAV1 that was distinct from the endogenous protein. We hypothesized that this HA-tagged pool of CAV1 would be subject to palmitoylation by DHHC7 and/or DHHC21. To test this, the cells were transfected with HA–CAV1 alone or co-transfected with HA–CAV1 and DHHC7, DHHC21, or DHHC10 and subjected to acyl–biotin exchange. We found that DHHC7 overexpression increased HA–CAV1 palmitoylation over that of the control (NT), but overexpression of DHHC21 or DHHC10 did not (Fig. 3, $F(3,20) = 8.4$, $p < 0.001$).

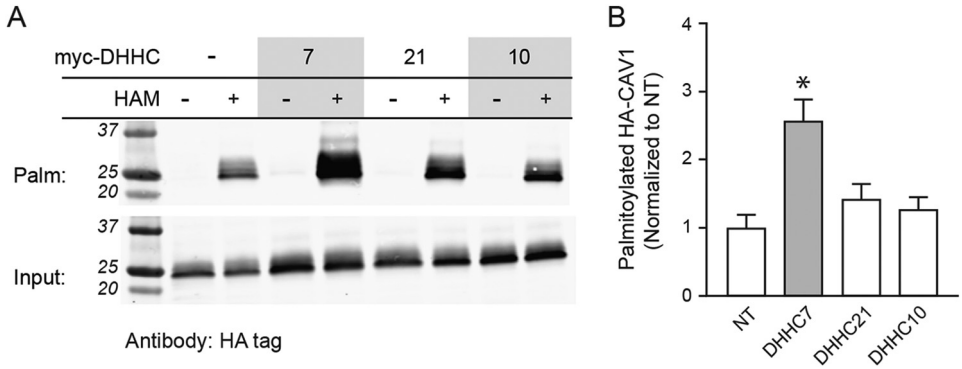

Figure 3. DHHC7 increased HA-tagged CAV1 palmitoylation. *A*, Western blotting indicating HA-tagged CAV1 exhibits increased palmitoylation (*Palm*) following overexpression of DHHC7, but not DHHC21 or DHHC10. *B*, average intensity of HA–CAV1 palmitoylation. *, $p < 0.001$ *versus* NT group. *HAM*, hydroxylamine.

Mutant HA–CAV1 is not palmitoylated, but still associates with DHHC7 and plasma membrane

To establish that DHHC7-mediated HA–CAV1 palmitoylation occurred at the expected cysteine residues, we created a mutant version of the HA–CAV1 plasmid in which all three of the putative palmitoylation sites were changed from cysteine to alanine, rendering the protein palmitoylation-null (Fig. 4*A*). No palmitoylation of this mutant (MT) HA–CAV1 was detected, even when DHHC7 was overexpressed (Fig. 4*B*), suggesting that DHHC7 increased CAV1 palmitoylation at the expected sites.

To further demonstrate that there were no gross abnormalities in the MT HA–CAV1 that would interfere with palmitoylation, such as abnormal protein folding, etc., we performed immunoprecipitation experiments to see whether it still associated with DHHC7 (Fig. 4*C*). Co-immunoprecipitation of CAV1 and DHHC7 was not interrupted, suggesting that altering these residues did not interfere with DHHC-substrate binding but only with palmitate attachment.

Palmitoylation also often plays an important role in the trafficking of proteins to the plasma membrane. Thus, although biochemical fractionation experiments have suggested that CAV1 palmitoylation is not necessary for association with caveolae- and lipid raft-associated fractions (20), we wanted to know whether imaging would reveal any palmitoylation-dependent changes in CAV1 trafficking. Consequently, we performed TIRF imaging of cells transfected with WT or MT CAV1 tagged with mNeonGreen to determine whether membrane localization of CAV1 depends on its palmitoylation. This revealed both WT and MT CAV1 at or near the membrane (*i.e.* within 100 nm) (Fig. 4*D*). No difference in TIRF fluorescence was observed when normalized to the total wide-field fluorescence (Fig. 4*E*, $t = 0.067$, $p = 0.95$). These findings support the conclusion that palmitoylation is not essential for the membrane targeting of CAV1.

Possible relationship between DHHC7 and DHHC21

Having demonstrated that overexpression of DHHC7 is *sufficient* to increase HA–CAV1 palmitoylation, we sought to determine whether DHHC7 is also *necessary* for CAV1 palmitoylation. To do so, we transfected HEK293 cells with siRNA targeting genes zDHHC7, zDHHC21, or a nontargeting siRNA, followed by overexpression of HA–CAV1 and ABE analysis (Fig. 5, *A* and *B*). Surprisingly, knockdown of DHHC7 (or DHHC21) did not cause a reduction in HA–CAV1 palmitoylation (Fig. 5*A*, $F(3,5) = 2.6$, $p = 0.17$). siRNA effectiveness and specificity were verified by qPCR (Fig. 5*B*; *, $p < 0.05$ compared with NT condition).

Because of the requirement for both DHHC7 and DHHC21 for membrane-initiated estradiol signaling, we considered the possibility of a cooperative interaction between DHHC7 and DHHC21 in regards to CAV1 palmitoylation. Thus, we transfected cells with siRNA targeting both DHHC7 and DHHC21 to see whether simultaneous reduction would alter CAV1 palmitoylation. Interestingly, following disruption of both DHHC7 and DHHC21, we observed a decrease in HA–CAV1 palmitoylation (Fig. 5*C*, $t(6) = 4.11$, $p = 0.006$), indicating a relationship or redundancy between these two enzymes in the context of CAV1 palmitoylation. Effectiveness of knockdown was again verified by qPCR (Fig. 5*D*; *, $p < 0.05$ compared with NT condition).

One explanation of why expression of both DHHC7 and DHHC21 must be compromised to decrease HA–CAV1 palmitoylation is that DHHC21 facilitates activity of DHHC7. To test this possibility, we examined whether siRNA knockdown of DHHC21 would eliminate the effect of DHHC7 overexpression (Fig. 6, *left panel*). As shown before, DHHC7 overexpression increased HA–CAV1 palmitoylation, but this was not affected by DHHC21 knockdown (Fig. 6, *right panel*; $F = 14.08$, $p < 0.01$; Tukey $p < 0.05$), suggesting that DHHC7 does not require DHHC21 to increase CAV1 palmitoylation.

Given that DHHC7 activity does not appear to depend on the presence of DHHC21, we wanted to know whether these two enzymes are localized to different cellular compartments in HEK293 cells. To address this, we transfected HEK293 cells with Myc-tagged DHHC7 or DHHC21 and immunostained cells for Myc tag expression and co-stained with markers for the Golgi apparatus and the nucleus. Confocal images revealed that DHHC7 expression was widespread, but DHHC21 expression appeared to be restricted to the Golgi apparatus (Fig. 7).

Discussion

The current understanding of the regulatory role palmitoylation plays in ER membrane trafficking and ER/mGluR sig-

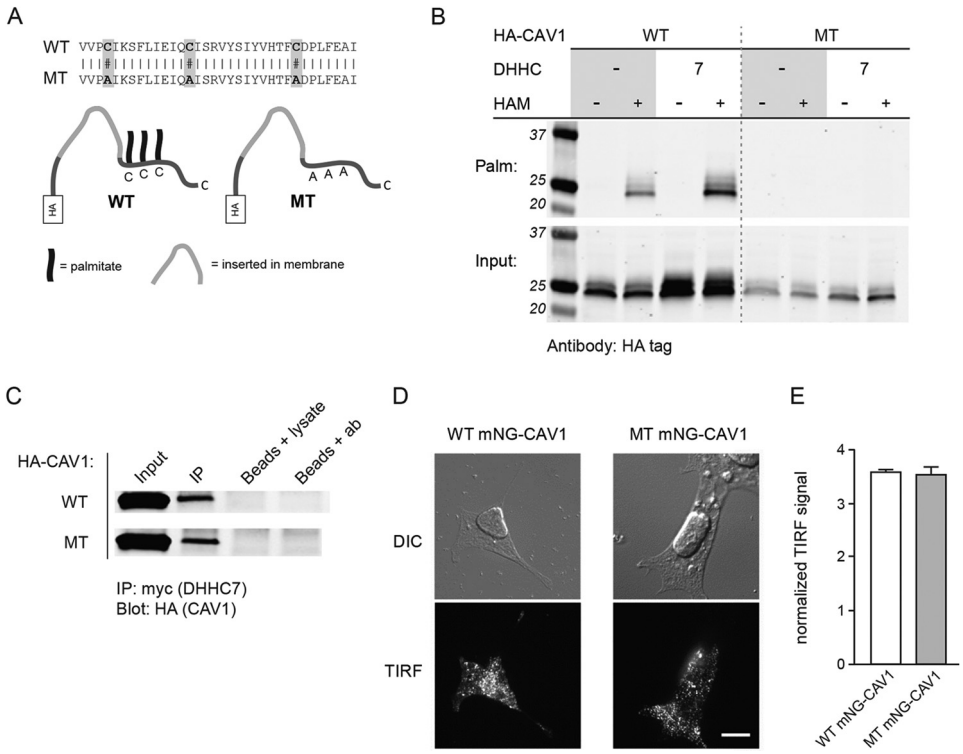

Figure 4. Palmitoylation-null CAV1 still associates with DHHC7 and the plasma membrane. *A*, amino acid sequence and protein schematic of WT and mutant palmitoylation-null (MT) HA-tagged CAV1. In the MT, all three cysteine residues found in WT CAV1 were changed to alanine. *B*, DHHC7 increased WT HA–CAV1 palmitoylation (*Palm*), whereas palmitoylation of MT HA–CAV1 was completely absent. *C*, mutation of HA–CAV1 did not affect co-immunoprecipitation with DHHC7. *D*, differential interference contrast (*DIC*) (*top panels*) and TIRF (*bottom panels*) imaging of HEK293 cells transfected with WT (*left panels*) or MT (*right panels*) mNeonGreen (*mNG*)-tagged CAV1 (mNG-CAV1). *Scale bar*, 10 μm. *E*, membrane localization of CAV1 was unaffected by palmitoylation state. *HAM*, hydroxylamine; *IP*, immunoprecipitation.

naling has thus far been limited by focusing solely on the ER, to the exclusion of other regulatory proteins involved in this mechanism of ER action. Although effector proteins downstream of mGluR activity are likely subject to palmitoylation activity as well, it is critical to understand potential post-translational modifications to the proteins that facilitate the ER/mGluR interaction in the first place. Our finding that the same DHHCs important for steroid receptor palmitoylation also affect CAV1 palmitoylation adds another layer of regulation to the ER/mGluR signaling model.

The finding that two DHHCs must be knocked down to decrease CAV1 palmitoylation suggests that there is some form of cooperation between DHHC7 and DHHC21. Perhaps one palmitoylates the other, or perhaps they are localized to different subcellular compartments, as the immunostaining presented here and elsewhere (14) suggest. Moreover, although it is clear that there is DHHC-substrate specificity, most protein substrates can be palmitoylated by more than one DHHC enzyme (27). This palmitoyl acyltransferase (PAT) redundancy may be particularly apparent when the substrate is overexpressed, which would explain why siRNA knockdown of both DHHC7 and DHHC21 was required here to decrease palmitoylation of overexpressed CAV1. An additional possibility is that these DHHCs can act as a functional heteromer. Lai and Linder (28) suggest that the oligomerization states of DHHC proteins affect their enzymatic activities. These alternative hypotheses await further study.

Our findings from TIRF imaging are also consistent with previous work indicating that palmitoylation does not affect CAV1 membrane trafficking (20). Importantly, the presence of non-palmitoylated CAV1 at or near the membrane does not indicate CAV1 function remains intact. For example, CAV1 must be palmitoylated to interact with G proteins (29). Moreover, because CAV1 is an important component of lipid rafts, changes in CAV1 palmitoylation could alter lipid raft dynamics and therefore signal transduction.

Additionally, the present work did not distinguish between the three palmitoylation sites on CAV1. Previous reports suggest that although CAV1 is palmitoylated at all three cysteine residues, it is primarily palmitoylated at cysteine 133 (20). It remains to be seen whether all three sites are palmitoylated by a single palmitoyl acyltransferase and whether there is any order or sequence to possible site-specific palmitoylation. This could contribute to cell sorting, trafficking, and lipid raft association (4, 30).

One goal of investigating the regulation of proteins involved in ER/mGluR signaling is to elucidate the mechanisms that confer sex specificity to this pathway. Estradiol activation of mGluR G-protein activity through membrane localized estrogen receptors is often restricted to females (but see Refs. 10 and 11). Because there are no obvious differences in ER (or mGluR) expression between males and females in brain regions that exhibit a female-only ER/mGluR signaling, we and others hypothesize that sex specificity may instead be explained by the

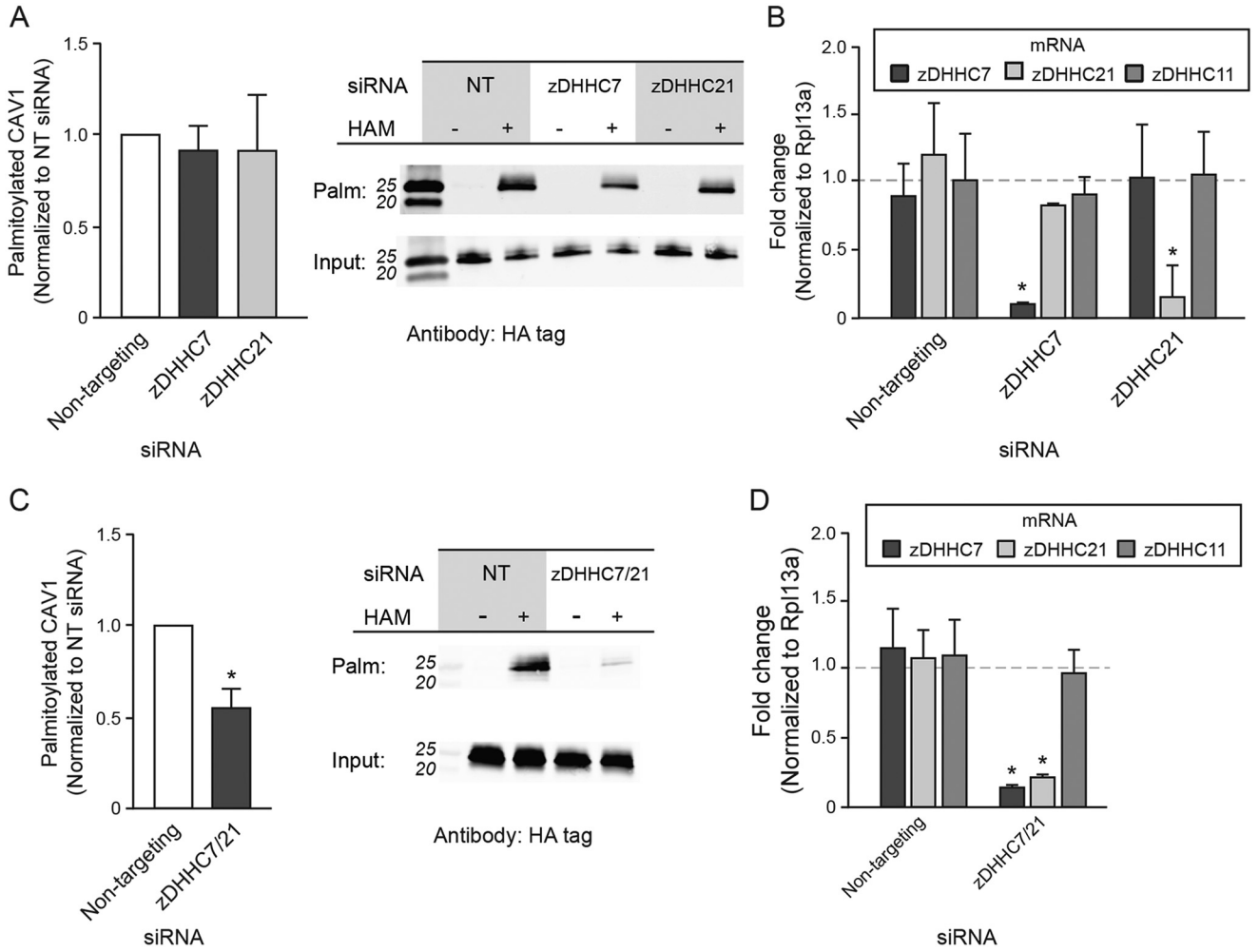

Figure 5. Simultaneous, but not single, knockdown of zDHHC7 and zDHHC21 decreases CAV1 palmitoylation. *A*, siRNAs targeting either zDHHC7 or zDHHC21 did not affect HA–CAV1 palmitoylation (*Palm*). *B*, qPCR validation of siRNA knockdown. *, $p < 0.05$ *versus* NT. *C*, simultaneous knockdown of zDHHC7 and zDHHC21 decreased HA–CAV1 palmitoylation. *, $p < 0.01$. *D*, qPCR validation of double siRNA knockdown. *, $p < 0.05$ *versus* NT. *HAM*, hydroxylamine.

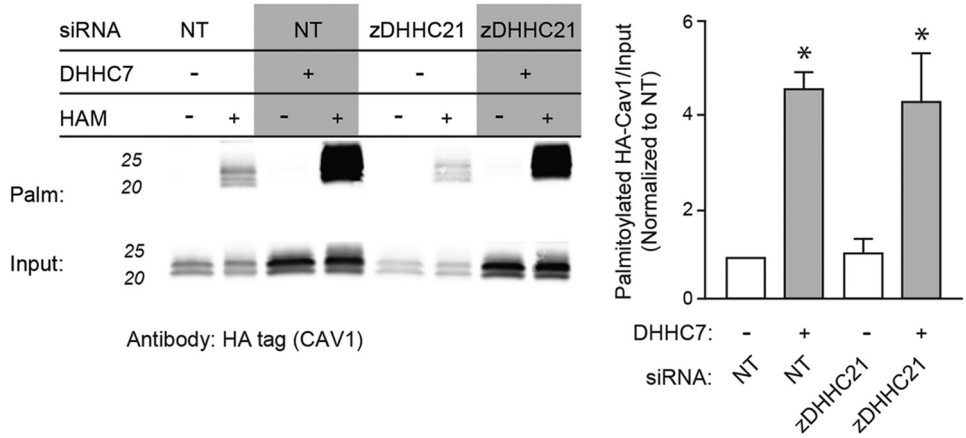

Figure 6. DHHC7-mediated CAV1 palmitoylation is not affected by knockdown of zDHHC21. *Left panel*, palmitoylation (*Palm*) of HA–CAV1 was increased by DHHC7, and was unaffected following disruption of DHHC21 expression. *Right panel*, average palmitoylation of HA–CAV1 with overexpression of DHHC7 and/or DHCC21 knockdown. *, $p < 0.05$ compared with basal palmitoylation controls. *HAM*, hydroxylamine.

regulatory processes that partner these signaling proteins together, such as palmitoylation and CAV1 association. Paradoxically, we have found that mRNA expression of both CAV1 and zDHHC7 is decreased in the hippocampus of adult female rats relative to males (31). No differences were observed in ER or zDHHC21 expression. In fact, no sex differences were observed in any of the remaining 22 palmitoyl acyltransferases. Because estrous cycles were not monitored during these studies, the possibility of hormonal regulation of CAV1 and/or DHHC7 expression remains. In fact, this may be a likely expla-

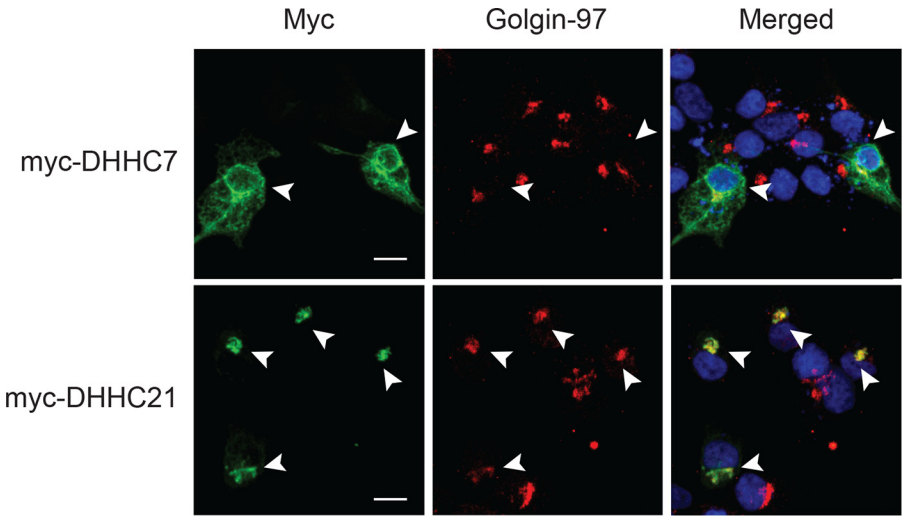

Figure 7. Differential subcellular localization of DHHC7 and DHHC21. Shown are confocal images of HEK293 cells transfected with Myc-tagged DHHC7 or DHHC21. Cellular expression of DHHC7 was widespread, whereas DHHC21 expression was restricted to the Golgi. *Green*, Myc tag; *red*, golgin-97; *blue*, nuclear counterstain. *Scale bar*, 10 μm.

nation based on findings from a variety of tissues that estradiol increases CAV1 expression, including endothelial cells (32), female mouse hypothalamus (33), female rat bladder (34), rat adipose tissue to a greater degree in females (35), and rat uterine tissue (36). Moreover, this could be a locus of intersection between classical estrogen receptor regulation of gene expression and ER/mGluR signaling. It remains to be seen whether or not DHHC7 expression is subject to estradiol regulation.

S-Palmitoylation is a powerful regulatory mechanism in large part because of its reversible nature. Indeed, many groups have reported activity-dependent fluctuations in palmitoylation that may contribute to signaling outcomes (1, 37–39). Dynamic ER palmitoylation has also been observed, with estradiol exposure decreasing ER palmitoylation in cancer cell lines (12) and hippocampal synaptosomes (40). However, our data support the previous findings from Parat and Fox that CAV1 palmitoylation is a relatively stable modification, at least in HEK293 cell lines (23). Accordingly, in addition to elucidating the functional importance of CAV1 palmitoylation for ER/mGluR and other signaling mechanisms, future work must consider the relevance of its permanence.

Dysregulation of CAV1 has been implicated in a wide array of disease processes, including various cancers (41), liver disease (42), chronic pain (43), neurodegeneration (44), and schizophrenia (45). CAV1 is likely to exert influence on these processes through its roles as both an organizer of signaling molecules and as a regulator of membrane dynamics and lipid raft domains. Consequently, palmitoylation and palmitoyl acyltransferases not only provide a potential target for cellular regulation of CAV1 with respect to estrogen receptor activity at the cell membrane but may also provide insight into how this cell signaling regulatory protein affects distinct cellular processes both in and out of the nervous system.

Experimental procedures

Estradiol-mediated CREB phosphorylation

Cell culture—Hippocampal neurons were cultured from female Sprague–Dawley rat pups at postnatal day 1 or 2 as described previously (6), in accordance and approval from the Institutional Animal Care and Use Committee at the University of Minnesota. Hippocampi were isolated in ice-cold modified Hanks' balanced salt solution containing 20% fetal bovine serum (Atlanta Biologicals) and 4.2 mM $NAHCO_3$ and 1 mM HEPES, pH 7.35, 300 mOsm. Tissue was then washed and subjected to a 5-min digestion in a trypsin solution with 137 mM NaCl, 5 mM KCl, 7 mM Na_2HPO_4, 25 mM HEPES, and 1500 units of DNase, pH 7.2, 300 mOsm. After additional washes, tissue was dissociated by trituration and pelleted twice by centrifugation. The cells were then plated on Matrigel-treated coverslips and incubated for 20 min at room temperature prior to the addition of 2 ml of minimum Eagle's medium (Invitrogen) with 28 mM glucose, 2.4 mM $NaHCO_3$, 0.0013 mM transferrin (Calbiochem, San Diego, CA), 2 mM glutamine, 0.0042 mM insulin, 1% B-27 (Invitrogen), and 10% fetal bovine serum (pH 7.35, 300 mOsm). 48 h after plating, 1 ml of medium was replaced with a solution containing 4 μM cytosine 1-β-D-arabinofuranoside to inhibit glial growth. The cells were fed 4 days later by replacement of 1 ml of medium. Gentamicin (2 μg/ml; Invitrogen) was added to all media solutions to eliminate bacterial growth.

Immunocytochemistry—Cell stimulations and immunocytochemistry were performed as described previously (6). Neurons (8–9 days *in vitro*) were pretreated in a Tyrode solution containing tetrodotoxin (1 μM) and APV (25 μM) for 2 h prior to a 5-min stimulation with 1 nM 17β-estradiol. Neurons were then fixed in ice-cold 4% paraformaldehyde (Electron Microscopy Sciences, Hatfield, PA) in PBS containing 4 mM EGTA and subsequently washed in PBS, permeabilized with 0.1% Triton X-100, washed again, and then blocked at 37 °C for 30 min in PBS plus 1% BSA and 2% goat serum (Jackson ImmunoResearch, West Grove, PA). The cells were stained with primary antibodies directed against serine 133–phosphorylated cAMP response element binding protein (pCREB; monoclonal, 1:1000; Upstate Biotechnology) and against microtubule-associated protein 2 (MAP2; polyclonal, 1:1000; Calbiochem). Alexa Fluor 488 and 635 secondary antibodies (Invitrogen) were used for visualization of MAP2 and pCREB, respectively. Coverslips

were washed and mounted using Citifluor (Ted Pella, Redding, CA). Nuclear fluorescence intensities for pCREB were acquired using a Leica DM5500Q confocal system and quantified with Leica LAS AF (version 1.9.0; Leica).

Neurons were selected randomly using MAP2 fluorescence, and images were captured through the approximate midline of each cell. For analysis, a region of interest was drawn around the nucleus of each neuron according to MAP2 staining, which allowed unbiased analysis of pCREB intensity. This was done by transferring the region of interest from the MAP2 image to the pCREB image and then measuring fluorescence intensities. Average pCREB fluorescence intensities within the nucleus were recorded (n = approximately 25 neurons/group). The background from a region of the image not containing pCREB fluorescence was subtracted from the average pCREB fluorescence.

Measurement of protein palmitoylation

Acyl–biotin exchange (ABE)—HEK293 cells (ATCC, Manassas, VA) were maintained at 37 °C, 5% CO_2 in Dulbecco's modified Eagle's medium supplemented with 1% penicillin/streptomycin and 5% fetal bovine serum. Acyl–biotin exchange was performed according to procedures outlined previously (37, 46, 47). HEK293 cells were lysed in buffer containing 150 mM NaCl, 50 mM Tris, pH 7.4, 5 mM EDTA, 0.2% Triton X-100, 10 mM NEM, and protease inhibitor mixture (Pierce) by sonication. Additional Triton X-100 was then added for a total concentration of 1.7%. Lysates were then mixed at 4 °C for 1 h and clarified at 12,000 × *g* for 10 min. Chloroform-methanol precipitation was performed, and then proteins were incubated with 50 mM NEM overnight to block free cysteine residues. Protein was again precipitated the following day and divided into two equal portions. One portion was incubated with 10 mM HPDP–biotin buffer containing hydroxylamine (1 h, room temperature) to cleave thioesterase bonds and replace palmitoyl groups with biotin. The remaining half was incubated with 10 mM HPDP–biotin (Life Technologies) without hydroxylamine as a control. Chloroform-methanol precipitation was again performed, and then samples were incubated with streptavidin–agarose beads (GE Healthcare) in lysis buffer (no NEM) overnight to capture biotin-labeled proteins. 10% of each sample portion was reserved prior to pulldown for use as input control. The following morning, the beads were washed four times with lysis buffer before proteins were eluted in Laemlli sample buffer (Bio-Rad) at 90 °C for 10 min. Eluted proteins and input controls were then subjected to SDS–PAGE (4–20% Mini-PROTEAN TGX precast gels; Bio-Rad) and Western blotting (nitrocellulose; Bio-Rad). The blots were blocked with Odyssey blocking buffer TBS (LI-COR, Lincoln, NE) and incubated overnight in primary antibody. The antibodies used were rabbit anti-CAV1 1:5000 (Abcam, Cambridge, MA; ab2910), goat anti-HA tag 1:5000 (Abcam, ab9134), mouse anti-HA tag 1:5000 (Abcam; ab18181), and mouse anti-Myc tag 1:5000 (Sigma; M4439). The blots were then washed in TBS + Tween and incubated with the appropriate fluorescent secondary antibodies (LI-COR). The blots were imaged and analyzed using Odyssey scanner and software (LI-COR). Palmitoylated proteins were normalized to their respective input control for data analysis.

Antibody validation—Tissue punches obtained from WT or CAV1 KO mice were homogenized with a bullet blender (Next Advance, Troy, NY) and lysed in radioimmune precipitation assay buffer supplemented with protease and phosphatase inhibitors. Equal protein was run on SDS–PAGE prior to Western blotting with 1:5000 dilution of rabbit anti-Cav1 (Abcam, *red*) and 1:20,000 mouse anti-GAPDH (Millipore, *green*). (Channels of two-color blot were merged and changed to gray scale using ImageJ.)

2-Bromopalmitate incubation

HEK293 cells were either treated overnight with 100 μM 2-Br (Sigma) prepared at 10 mM in DMSO and diluted to final concentration in culture media or treated with vehicle alone. ABE was performed as described above. Following Western blotting for CAV1 as described above, the blots were stripped with 1× NewBlot IR stripping buffer (LI-COR) for 15 min, washed, blocked, and probed for Ras (rabbit anti-pan-Ras, 1:5000, 52939; Abcam).

Immunoprecipitation

The cells were lysed in ice-cold buffer containing 150 mM NaCl, 50 mM Tris, pH 8, 1% NP-40, and protease and phosphatase inhibitors (Pierce). Equal amounts of lysate per sample were incubated in anti-Myc antibody (Sigma; M4439) in PBS for 1 h at 4 °C. Dynabeads G (Novex; Invitrogen) were then added, and the incubation was continued overnight. The beads were washed the following morning before elution in 2× Laemlli buffer (Bio-Rad). Eluted proteins were then subjected to SDS–PAGE and Western blotting as described above.

Plasmid and siRNA transfection

CAV1 was inserted into a pCMV-HA vector (Addgene, 32530) using PCR-based cloning. mNeongreen-CAV1 was obtained from Allele Biotechnology (San Diego, CA). DHHC plasmids were a gift from the Bamji Lab (University of British Columbia). Site-directed mutagenesis was performed using QuikChange Lightning Multi (Agilent, Santa Clara, CA). The cells were transfected using Xtremegene HP (Roche Applied Science).

siRNAs were purchased from GE Healthcare Dharmacon, specifically ON-TARGETplus Nontargeting or SMARTpool. These contain a mixture of four distinct siRNAs against each target. The cells were transfected with 50 nM siRNA using Dharmafect (GE Healthcare). Knockdown was verified using qPCR as described previously (7). Briefly, RNA was extracted from cells using RNeasy kit (Qiagen), followed by cDNA synthesis from 1 μg of RNA using Roche transcriptor first strand cDNA synthesis kit. qPCR was performed on Lightcycler 480 (Roche) using Lightcycler 480 SYBR Green I Master. The primers used were RPL13A, 5′-TACTTCACTGTTTAGCCACGAT-3′ and 5′-CGAAGATGGCGGAGGTG-3′; zDHHC7, 5′-GTCCTGATGGCTGCATGA-3′ and 5′-GACAGTATGCACCTTAAGATCCT-3′; zDHHC11, 5′GGATCACAGGGGCACCT-3′ and 5′-ATGGCACAGGAAGCAGATG-3′; and zDHHC21, 5′-CACTTGTTACATAATTCCCAGAACT-3′ and 5′-GGCCTCCATAACTGATCCAG-3′. The results were analyzed using the ΔΔCT method (48).

TIRF imaging

Immunocytochemistry—HEK293 cells were transiently transfected with pMNG-CAV1-C10 or pMNG-CAV1-MT with Lipofectamine 3000 according to the manufacturer's suggestions (Invitrogen). The next day, the cells were scraped from flasks and seeded onto 35-mm imaging dishes equipped with #1.5 coverglass (Eppendorf North America, Hauppauge, NY). Two days post-transfection, the cell growth medium was removed, and the cells were fixed using a solution of 2.0% formaldehyde, 7% picric acid in Tris and PBS (a 1:1 mixture of TBS and PBS), pH 6.9, for 2 min at room temperature. The fixative solution was drawn off and replaced with a solution of 4% formaldehyde, 14% picric acid in PBS, pH 6.9, for 5–10 min at room temperature. The fixative was removed from the cells and washed several times with TBS. The cells were stained using a 1:1000 dilution of rabbit anti-CAV1 (Abcam) in TBS containing 0.2% Triton X-100 (Fisher Scientific) and 0.2% Tween 20 (Sigma) for 4 h to overnight at room temperature. The cells were washed for 1 h with TBS and then stained with 1:1000 donkey anti-rabbit Alexa 568 in the TBS/Triton/Tween diluent for 2 h at room temperature. The cells were washed for 1 h with TBS, and the solution was replaced with DMEM containing antibiotics (Anti-Anti; Invitrogen) to inhibit bacterial growth during storage before imaging at 4 °C.

Total internal reflectance fluorescence (TIRF) microscopy—TIRF imaging was performed using a Zeiss Axio Observer Z1 inverted microscope (Carl Zeiss Microscopy, Thornwood, NY) equipped with a 100×/1.46na oil objective and Zen2 acquisition and analysis software. Wide-field images were obtained by first locating endogenous caveolin 1 that was visualized using immunocytochemistry and Alexa 568 fluorescence. After a cell was identified and imaged using differential interference contrast optics, the 561-nm laser was engaged at 10% power, and focusing from the coverglass into the cell, at the first instance of in-focused fluorescence of caveolin 1 (Alexa 568 –stained structures), a wide-field image was acquired. The 488-nm laser was then engaged at 1% power, and a wide-field image of mNeongreen fluorescence was obtained. The microscope was then switched to TIRF mode, the optimal angle of incidence was determined (typically the angle was ~65°), and images were obtained. The images were converted to TIFF using the Fiji build (version 2) of the freely available ImageJ software (ImageJ.net) and were minimally processed (adjusted contrast, brightness, and unsharp mask) using Photoshop software (CS5.1; Adobe Systems Inc.). For analysis, the cells were traced in Fiji, and mean TIRF fluorescence was normalized to the total wide-field fluorescence. Log transformation was performed to correct for unequal variances prior to quantification and use of the unpaired *t* test.

Subcellular localization immunocytochemistry

HEK293 cells plated on poly-D-lysine–coated coverslips in 6-well tissue culture plates were transfected with 0.5 μg of plasmid DNA (DHHC7 or DHHC21) using XtremeGENE HP (Roche). 24 h later, the cells were fixed, permeabilized, and blocked using reagents from Image-iT fixation/permeabilization kit (Thermo Fisher). Briefly, the cells were fixed for 15 min at room temperature in 4% formaldehyde, washed in PBS and then permeabilized for 15 min at room temperature with 0.5% Triton X-100. The cells were again washed and then blocked in 3% BSA for 1 h at room temperature. The cells were then incubated for 24 h at 4 °C in primary antibodies diluted in BlockAid (Thermo Fisher) at 1:200 (rabbit anti-Myc tag 71D10; CST; and mouse anti-Golgin-97 CDF4; Thermo Fisher). Following PBS washes, the cells were then incubated in secondary AlexaFluor+ antibodies diluted 1:1000 in BlockAid for 1 h at room temperature (goat anti-mouse 488, A32723; goat anti-rabbit 555, A32732; Thermo Fisher). The cells were again washed and then subjected to a 5-min incubation with 5 μM DRAQ5 nuclear stain (CST). Coverslips were washed a final time and then inverted into ProLong Diamond antifade mountant (Thermo Fisher) on slides for visualization. Confocal images were taken using a Leica DM5500Q confocal system and Leica LAS X software. Z stacks were taken through the cell using a 40× objective plus 3× digital zoom. Laser power, emission filters, and gain were set to optimize dynamic range. Fiji software was used to pseudocolor, minimally process, and create maximum projections of Z-stack images.

Statistical analysis

Data generated by Western blotting and immunocytochemistry were analyzed by one-way analysis of variance or unpaired *t* test, as appropriate. All experiments were repeated at least three times, with exemplar blots shown in figures. Tukey's tests were used for all post hoc analyses between treatment groups, with a determination of $p < 0.05$ for significance. Graphs are presented as means ± S.E.

Author contributions—K. R. T. E. and P. G. M. conceptualization; K. R. T. E., S. P. S., S. A. S., and J. M. investigation; K. R. T. E. writing-original draft; K. M. W. methodology; K. M. W., M. D., and P. G. M. writing-review and editing; P. G. M. supervision.

Acknowledgments—We thank Kellie Gross for suggestions on this work and Julia Dworsky for qPCR assistance.

References

1. Fukata, Y., Dimitrov, A., Boncompain, G., Vielemeyer, O., Perez, F., and Fukata, M. (2013) Local palmitoylation cycles define activity-regulated postsynaptic subdomains. *J. Cell Biol.* **202,** 145–161 CrossRef Medline
2. Blaskovic, S., Adibekian, A., Blanc, M., and van der Goot, G. F. (2014) Mechanistic effects of protein palmitoylation and the cellular consequences thereof. *Chem. Phys. Lipids.* **180,** 44–52 CrossRef Medline
3. Fukata, Y., and Fukata, M. (2010) Protein palmitoylation in neuronal development and synaptic plasticity. *Nat. Rev. Neurosci.* **11,** 161–175 CrossRef Medline
4. Greaves, J., and Chamberlain, L. H. (2007) Palmitoylation-dependent protein sorting. *J. Cell Biol.* **176,** 249–254 CrossRef Medline
5. Greaves, J., Prescott, G. R., Gorleku, O. A., and Chamberlain, L. H. (2009) The fat controller: roles of palmitoylation in intracellular protein trafficking and targeting to membrane microdomains. *Mol. Membr. Biol.* **26,** 67–79 CrossRef Medline
6. Boulware, M. I., Weick, J. P., Becklund, B. R., Kuo, S. P., Groth, R. D., and Mermelstein, P. G. (2005) Estradiol activates group I and II metabotropic glutamate receptor signaling, leading to opposing influences on cAMP response element-binding protein. *J. Neurosci.* **25,** 5066–5078 CrossRef Medline

7. Meitzen, J., Luoma, J. I., Boulware, M. I., Hedges, V. L., Peterson, B. M., Tuomela, K., Britson, K. A., and Mermelstein, P. G. (2013) Palmitoylation of estrogen receptors is essential for neuronal membrane signaling. *Endocrinology* **154,** 4293–4304 CrossRef Medline
8. Tonn Eisinger, K. R., Larson, E. B., Boulware, M. I., Thomas, M. J., and Mermelstein, P. G. (2018) Membrane estrogen receptor signaling impacts the reward circuitry of the female brain to influence motivated behaviors. *Steroids* **133,** 53–59 Medline
9. Cornil, C. A., Ball, G. F., and Balthazart, J. (2012) Rapid control of male typical behaviors by brain-derived estrogens. *Front. Neuroendocrinol.* **33,** 425–446 CrossRef Medline
10. Seredynski, A. L., Balthazart, J., Ball, G. F., and Cornil, C. A. (2015) Estrogen receptor β activation rapidly modulates male sexual motivation through the transactivation of metabotropic glutamate receptor 1a. *J. Neurosci.* **35,** 13110–13123 CrossRef Medline
11. Hedges, V. L., Chen, G., Yu, L., Krentzel, A. A., Starrett, J. R., Zhu, J.-N., Suntharalingam, P., Remage-Healey, L., Wang, J.-J., Ebner, T. J., and Mermelstein, P. G. (2018) Local estrogen synthesis regulates parallel fiber–Purkinje cell neurotransmission within the cerebellar cortex. *Endocrinology* **159,** 1328–1338 CrossRef Medline
12. Acconcia, F., Ascenzi, P., Fabozzi, G., Visca, P., and Marino, M. (2004) *S*-Palmitoylation modulates human estrogen receptor-α functions. *Biochem. Biophys. Res. Commun.* **316,** 878–883 CrossRef Medline
13. Pedram, A., Razandi, M., Sainson, R. C., Kim, J. K., Hughes, C. C., and Levin, E. R. (2007) A conserved mechanism for steroid receptor translocation to the plasma membrane. *J. Biol. Chem.* **282,** 22278–22288 CrossRef Medline
14. Pedram, A., Razandi, M., Deschenes, R. J., and Levin, E. R. (2012) DHHC-7 and -21 are palmitoylacyltransferases for sex steroid receptors. *Mol. Biol. Cell* **23,** 188–199 CrossRef Medline
15. Boulware, M. I., Kordasiewicz, H., and Mermelstein, P. G. (2007) Caveolin proteins are essential for distinct effects of membrane estrogen receptors in neurons. *J. Neurosci.* **27,** 9941–9950 CrossRef Medline
16. Christensen, A., and Micevych, P. (2012) CAV1 siRNA reduces membrane estrogen receptor-α levels and attenuates sexual receptivity. *Endocrinology* **153,** 3872–3877 CrossRef Medline
17. Razandi, M., Oh, P., Pedram, A., Schnitzer, J., and Levin, E. R. (2002) ERs associate with and regulate the production of caveolin: implications for signaling and cellular actions. *Mol. Endocrinol.* **16,** 100–115 CrossRef Medline
18. Hansen, C. G., and Nichols, B. J. (2010) Exploring the caves: cavins, caveolins and caveolae. *Trends Cell Biol.* **20,** 177–186 CrossRef Medline
19. Stern, C. M., and Mermelstein, P. G. (2010) Caveolin regulation of neuronal intracellular signaling. *Cell Mol. Life Sci.* **67,** 3785–3795 CrossRef Medline
20. Dietzen, D. J., Hastings, W. R., and Lublin, D. M. (1995) Caveolin is palmitoylated on multiple cysteine residues: palmitoylation is not necessary for localization of caveolin to caveolae. *J. Biol. Chem.* **270,** 6838–6842 CrossRef Medline
21. Luoma, J. I., Boulware, M. I., and Mermelstein, P. G. (2008) Caveolin proteins and estrogen signaling in the brain. *Mol. Cell Endocrinol.* **290,** 8–13 CrossRef Medline
22. Razani, B., Engelman, J. A., Wang, X. B., Schubert, W., Zhang, X. L., Marks, C. B., Macaluso, F., Russell, R. G., Li, M., Pestell, R. G., Di Vizio, D., Hou, H., Jr., Kneitz, B., Lagaud, G., Christ, G. J., *et al.* (2001) Caveolin-1 null mice are viable but show evidence of hyperproliferative and vascular abnormalities. *J. Biol. Chem.* **276,** 38121–38138 Medline
23. Parat, M.-O., and Fox, P. L. (2001) Palmitoylation of caveolin-1 in endothelial cells is post-translational but irreversible. *J. Biol. Chem.* **276,** 15776–15782 CrossRef Medline
24. Eisenberg, S., Laude, A. J., Beckett, A. J., Mageean, C. J., Aran, V., Hernandez-Valladares, M., Henis, Y. I., and Prior, I. A. (2013) The role of palmitoylation in regulating Ras localization and function. *Biochem. Soc. Trans.* **41,** 79–83 CrossRef Medline
25. Hancock, J. F., Magee, A. I., Childs, J. E., and Marshall, C. J. (1989) All ras proteins are polyisoprenylated but only some are palmitoylated. *Cell* **57,** 1167–1177 CrossRef Medline
26. Rocks, O., Peyker, A., Kahms, M., Verveer, P. J., Koerner, C., Lumbierres, M., Kuhlmann, J., Waldmann, H., Wittinghofer, A., and Bastiaens, P. I. (2005) An acylation cycle regulates localization and activity of palmitoylated Ras isoforms. *Science* **307,** 1746–1752 CrossRef Medline
27. Fukata, Y., Murakami, T., Yokoi, N., and Fukata, M. (2016) Local palmitoylation cycles and specialized membrane domain organization. In *Current Topics in Membranes* (Bennett, V., ed) pp. 97–141, Academic Press, Orlando, FL
28. Lai, J., and Linder, M. E. (2013) Oligomerization of DHHC protein *S*-acyltransferases. *J. Biol. Chem.* **288,** 22862–22870 CrossRef Medline
29. Galbiati, F., Volonte, D., Meani, D., Milligan, G., Lublin, D. M., Lisanti, M. P., and Parenti, M. (1999) The dually acylated NH_2-terminal domain of Gi1α is sufficient to target a green fluorescent protein reporter to caveolin-enriched plasma membrane domains. *J. Biol. Chem.* **274,** 5843–5850 CrossRef Medline
30. Levental, I., Lingwood, D., Grzybek, M., Coskun, U., Simons, K. (2010) Palmitoylation regulates raft affinity for the majority of integral raft proteins. *Proc. Natl. Acad. Sci.* **107,** 22050–22054 CrossRef Medline
31. Meitzen, J., Britson, K. A., Tuomela, K., and Mermelstein, P. G. (2017) The expression of select genes necessary for membrane-associated estrogen receptor signaling differ by sex in adult rat hippocampus. *Steroids* pii, S0039-128X(17)30179-4 CrossRef Medline
32. Jayachandran, M., Hayashi, T., Sumi, D., Iguchi, A., and Miller, V. M. (2001) Temporal effects of 17β-estradiol on caveolin-1 mRNA and protein in bovine aortic endothelial cells. *Am. J. Physiol. Heart Circ. Physiol.* **281,** H1327–H1333 CrossRef Medline
33. Zschocke, J., Manthey, D., Bayatti, N., van der Burg, B., Goodenough, S., and Behl, C. (2002) Estrogen receptor α-mediated silencing of caveolin gene expression in neuronal cells. *J. Biol. Chem.* **277,** 38772–38780 CrossRef Medline
34. Zhu, Q., Resnick, N. M., Elbadawi, A., and Kuchel, G. A. (2004) Estrogen and postnatal maturation increase caveolar number and caveolin-1 protein in bladder smooth muscle cells. *J. Urol.* **171,** 467–471 Medline
35. Mukherjee, R., Kim, S. W., Choi, M. S., and Yun, J. W. (2014) Sex-dependent expression of caveolin 1 in response to sex steroid hormones is closely associated with development of obesity in rats. *PLoS One* **9,** e90918 CrossRef Medline
36. Turi, A., Kiss, A. L., and Müllner, N. (2001) Estrogen downregulates the number of caveolae and the level of caveolin in uterine smooth muscle. *Cell Biol. Int.* **25,** 785–794 CrossRef Medline
37. Woolfrey, K. M., Sanderson, J. L., and Dell'Acqua, M. L. (2015) The palmitoyl acyltransferase DHHC2 regulates recycling endosome exocytosis and synaptic potentiation through palmitoylation of AKAP79/150. *J. Neurosci.* **35,** 442–456 CrossRef Medline
38. Brigidi, G. S., Sun, Y., Beccano-Kelly, D., Pitman, K., Mobasser, M., Borgland, S. L., Milnerwood, A. J., and Bamji, S. X. (2014) Palmitoylation of δ-catenin by DHHC5 mediates activity-induced synapse plasticity. *Nat. Neurosci.* **17,** 522–532 CrossRef Medline
39. Globa, A. K., and Bamji, S. X. (2017) Protein palmitoylation in the development and plasticity of neuronal connections. *Curr. Opin. Neurobiol.* **45,** 210–220 CrossRef Medline
40. Tabatadze, N., Smejkalova, T., and Woolley, C. S. (2013) Distribution and posttranslational modification of synaptic ERα in the adult female rat hippocampus. *Endocrinology* **154,** 819–830 CrossRef Medline
41. Chatterjee, M., Ben-Josef, E., Thomas, D. G., Morgan, M. A., Zalupski, M. M., Khan, G., Robinson, C. A., Griffith, K. A., Chen, C.-S., Ludwig, T., Bekaii-Saab, T., Chakravarti, A., and Williams, T. M. (2015) Caveolin-1 is associated with tumor progression and confers a multi-modality resistance phenotype in pancreatic cancer. *Sci. Rep.* **5,** 10867 CrossRef Medline
42. Fernandez-Rojo, M. A., and Ramm, G. A. (2016) Caveolin-1 function in liver physiology and disease. *Trends Mol. Med.* **22,** 889–904 CrossRef Medline
43. Yang, J.-X., Hua, L., Li, Y.-Q., Jiang, Y.-Y., Han, D., Liu, H., Tang, Q.-Q., Yang, X.-N., Yin, C., Hao, L.-Y., Yu, L., Wu, P., Shao, C.-J., Ding, H.-L., Zhang, Y.-M., *et al.* (2015) Caveolin-1 in the anterior cingulate cortex modulates chronic neuropathic pain via regulation of NMDA receptor 2B subunit. *J. Neurosci.* **35,** 36–52 CrossRef Medline

44. Head, B. P., Peart, J. N., Panneerselvam, M., Yokoyama, T., Pearn, M. L., Niesman, I. R., Bonds, J. A., Schilling, J. M., Miyanohara, A., Headrick, J., Ali, S. S., Roth, D. M., Patel, P. M., and Patel, H. H. (2010) Loss of caveolin-1 accelerates neurodegeneration and aging. *PLoS One* **5,** e15697 CrossRef Medline
45. Kassan, A., Egawa, J., Zhang, Z., Almenar-Queralt, A., Nguyen, Q. M., Lajevardi, Y., Kim, K., Posadas, E., Jeste, D. V., Roth, D. M., Patel, P. M., Patel, H. H., and Head, B. P. (2017) Caveolin-1 regulation of disrupted-in-schizophrenia-1 as a potential therapeutic target for schizophrenia. *J. Neurophysiol.* **117,** 436–444 Medline
46. Brigidi, G. S., and Bamji, S. X. (2013) Detection of protein palmitoylation in cultured hippocampal neurons by immunoprecipitation and acyl-biotin exchange (ABE). *J. Vis. Exp.* **18,** 50031
47. Kang, R., Wan, J., Arstikaitis, P., Takahashi, H., Huang, K., Bailey, A. O., Thompson, J. X., Roth, A. F., Drisdel, R. C., Mastro, R., Green, W. N., Yates, J. R., 3rd, Davis, N. G., and El-Husseini, A. (2008) Neural palmitoyl-proteomics reveals dynamic synaptic palmitoylation. *Nature* **456,** 904–909 CrossRef Medline
48. Schmittgen, T. D., and Livak, K. J. (2008) Analyzing real-time PCR data by the comparative C_T method. *Nat. Protoc.* **3,** 1101–1108 CrossRef Medline